

# Testing of the MESSENGER Spacecraft Phased-Array Antenna

Robert E. Wallis, Jonathan R. Bruzzi, and Perry M. Malouf

The Johns Hopkins University  
Applied Physics Laboratory  
Laurel, Maryland 20723-6099  
240-228-3836  
robert.wallis@jhuapl.edu

## ABSTRACT

**The MESSENGER spacecraft, designed to orbit the planet Mercury, will use the first electronically scanned phased-array antenna for a deep-space telecommunication application. Two lightweight phased-arrays, mounted on opposite sides of the spacecraft, provide the high-gain downlink coverage.**

**Techniques for measurement of the phased-array antenna system include ambient temperature measurements in a compact antenna range, thermal vacuum testing, and spacecraft level testing. There have been two novel developments in the characterization of the phased-array system. The first is a “gain envelope” response, which is a measurement of the gain of the array at the intended scan angle as the array is electrically scanned in 1° increments. This response was produced through a combination of hardware and test software to synchronize the gain measurement with the mechanical and electrical scanning. The second is a phase steering verification test that utilizes couplers in each steered element in conjunction with previously measured element patterns to confirm that the antenna beam is steered properly. This method allows functional verification of the phased-array system while radiating into an RF absorber-lined hat during spacecraft-level tests.**

**Keywords: Antenna measurements, Phased-array**

## 1. Introduction

Mercury Surface, Space ENvironment, GEochemistry, and Ranging (MESSENGER) is the latest NASA Discovery mission [1,2,3] managed by The Johns Hopkins University Applied Physics Laboratory (JHU/APL). MESSENGER is a mission to orbit the least explored terrestrial planet, Mercury. MESSENGER's high-data-rate downlink will use the first electronically scanned phased-array antenna for a deep-space telecommunication application. MESSENGER is

scheduled to launch in August 2004 and to be inserted into Mercury orbit in March 2011. The first spacecraft to orbit Mercury, MESSEGER will gather science data for one year and transmit it back to Earth.

The spacecraft uses a fixed sunshade to maintain the interior of the spacecraft near 25°C despite the fact that the solar intensity in Mercury orbit can be as large as 11 times the intensity seen at Earth. The severe thermal environment requires that the attitude control system orients the spacecraft with the sunshade always facing the Sun. Because of this orientation and the geometry associated with an inner planet mission, the Earth may be in any direction around the spacecraft in a plane aligned with the ecliptic. The restriction in spacecraft orientation precludes the use of a fixed antenna and spacecraft maneuvering to achieve Earth pointing, but rotation about the spacecraft-Sun line is still permitted.

Although one-dimensional electronically scanned antennas (1-D ESA) and gimbaled-dish antennas both provide high gain with low mass; the 1-D ESA requires no moving parts, and offers graceful degradation, more packaging flexibility, and high operating temperature. In addition, the extreme thermal environment precludes the use of active semiconductors directly behind the radiating elements. Since the uplink data rate is typically very low, the phased-array is needed for high-data-rate downlink only, which allows the use of a narrowband antenna.

Two lightweight phased-arrays, positioned on opposite sides of the spacecraft, are used for the high-gain downlink. Each phased-array antenna is electronically steered over a  $\pm 45^\circ$  range. One-dimensional steering, in combination with spacecraft rotation, provides antenna coverage for all Sun-Earth-spacecraft angles. Figure 1 shows the coverage area for the array antennas relative to the spacecraft orientation.

The phased-array antenna consists of an array of eight slotted waveguides and is shown in Figure 2. This antenna and the novel approach developed to produce circular polarization are described elsewhere [4]. The array 3 dB beam widths are roughly  $2^\circ$  in the narrow plane and  $12^\circ$  in the broad plane. The array is scanned in

the plane of the broad beam to minimize the number of cables and phase-shifter modules compared with narrow beam scanning. In addition broad beam scanning results in less pointing loss due to phase errors. Medium-gain (fanbeam) and low-gain antennas are used for uplink and low-gain downlink during cruise phase and emergency. The RF Telecommunication system, including the other antennas, has been previously described [5,6].

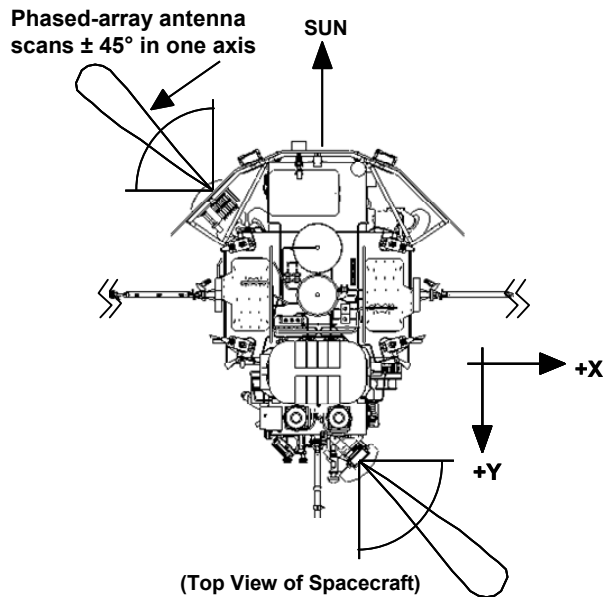


**Figure 1 Phased-Array Antenna Coverage**



**Figure 2 Flight Phased-Array and Fanbeam Antenna Assembly**

## 2. Component-Level Testing

### Pattern Measurement Facility

Direct measurements of the phased-array antenna gain were made using the JHU/APL indoor Compact Antenna Range. The facility utilizes a network analyzer in conjunction with a large broadband reflector, broadband feed horn, and RF switch to capture both the horizontally and vertically polarized radiation from an antenna under

test (AUT) in an otherwise anechoic chamber. The AUT is placed in the “quiet zone” of the chamber, where the broadband reflector produces a uniform phase front. A pair of mechanical stepper motors rotates the AUT in elevation and azimuth within the quiet zone as the network analyzer sweeps across a frequency band of interest, measuring the magnitude and phase of the signal returned across the compact range. Real-time digital processing performs a time-gating function to eliminate multipath reflections from the measurement. The circularly-polarized far-field radiation pattern is computed through post-processing and referenced to a separate measurement of a standard gain horn to determine the absolute gain of the AUT (magnitude and phase) versus mechanical scan angle.

To measure the gain of the phased-array antenna without requiring the flight Solid State Power Amplifiers (SSPAs), a set of eight, 4-bit commercial phase shifters was used. Each phase-shifter was calibrated for all phase states to determine the lookup table with which to test the phased-array. The radiated phases of the individual antenna sticks were also measured at boresight and taken into account in creating the optimal lookup table. The calibration also provided a measure of the loss introduced by the phase shifters themselves. This loss could then be subtracted out for a given state of the phase shifters in order to determine the gain of the phased-array alone.

A scheme was developed to expedite the process of measuring the antenna gain at every degree of electrical scan by interfacing the Compact Antenna Range software with the phase-shifter control software. Antenna gain was measured at the intended scan angle as the array was electronically steered in 1° increments between -60° and +60° from the broadside direction. This procedure allowed electrically scanned “gain envelopes” to be determined relatively quickly.

### Pattern Measurements

A set of antenna gain patterns was measured for each phased-array antenna. This set includes a gain envelope of the eight-stick full array and the two four-stick half arrays, the narrowbeam pattern for the broadside steered beam, as well as the broadbeam pattern at every 15° of electrical scan between -45° and +45° from the broadside direction. Figure 3 shows these measured broadbeam patterns, at a frequency of 8.432 GHz, overlaid with the gain envelope pattern as a function of scan angle.

Because the antenna is a narrow-band design it is sensitive to thermal-expansion-driven dimensional changes. The frequency at which the spacing of the antenna slots is a half-guide wavelength decreases with increasing temperature according to coefficient of thermal expansion (CTE) of the aluminum waveguide. This effect produces an equivalence between temperature and frequency such that an antenna’s frequency response can

be used to predict its thermal response. All pattern measurements include data across a frequency range that encompassed the operating temperature range of the antenna (-30° to +300°C). A typical frequency response is shown in Figure 4. The equivalent temperature for a fixed frequency downlink of 8.432 GHz is labeled along the X axis. Note that the gain is peaked for a downlink frequency of 8.432 GHz and a temperature of approximately 350°C, consistent with MESSENGER’s expected environment.

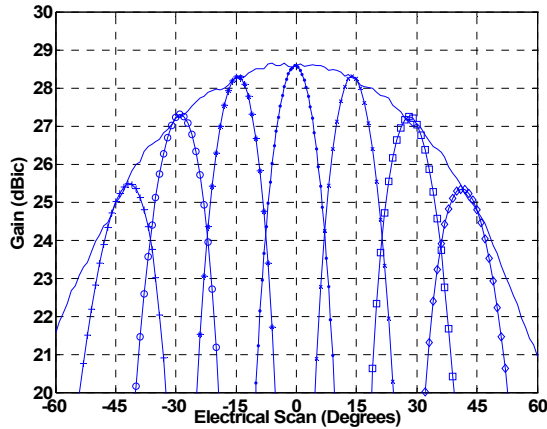


**Figure 3 Gain Envelope with Scan Patterns Overlaid**

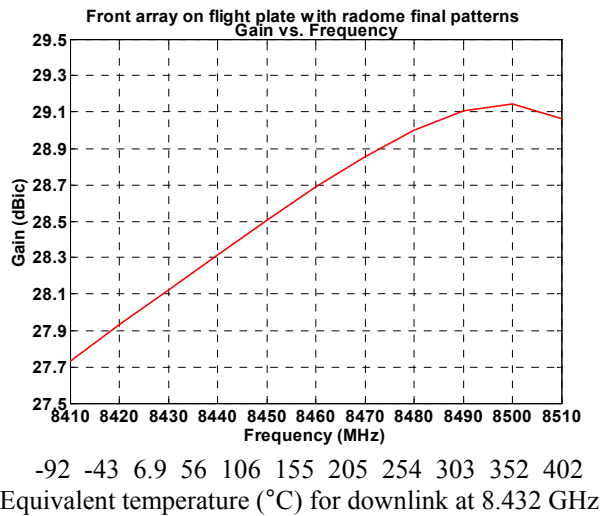


**Figure 4 Antenna Frequency / Temperature Response**

Antenna-Level Flight Qualification

Throughout the flight qualification process, a subset of the aforementioned patterns was repeatedly measured along with return loss and a set of individual antenna stick element patterns. These measurements provided an assessment of the repeatability of the measurements and the effect of flight environment testing on the antennas.

The overall flow for the flight antenna qualification is shown in Figure 5. Initial pattern and return loss measurements were made prior to thermal vacuum (TVAC) testing with the antenna sticks mounted to a thermal test plate required to raise the temperature of the antenna to 300°C. Several heaters and blankets were employed, as shown in Figure 6, to simulate the expected thermal environments for the different parts of the antenna assembly. Return loss was monitored throughout TVAC temperature cycling. Pattern and return loss measurements were measured following TVAC testing. The antennas were then assembled to their flight mounting plates.

The front antenna underwent testing at NASA Glenn Research Center where the antenna was exposed to the equivalent of 11 Suns and entered a single TVAC cycle test. Final antenna patterns were taken prior to vibration. Because the repeatability of the antenna gain measurements made in the Compact Antenna Range was less than 0.1 dB, we were able to detect slight changes in gain. One such change in antenna gain was noted and tracked to antenna mounting screws that had loosened during TVAC testing. The screws were then torqued and all subsequent measurements of gain repeated within the facility’s measurement repeatability. Return loss was monitored throughout vibration testing. Following vibration testing, the final set of return loss measurements was taken. Prior to installation of the antennas on the spacecraft, the antennas were electrically integrated with the SSPAs to verify the end-to-end system performance (gain and Effective Isotropic Radiation Power).

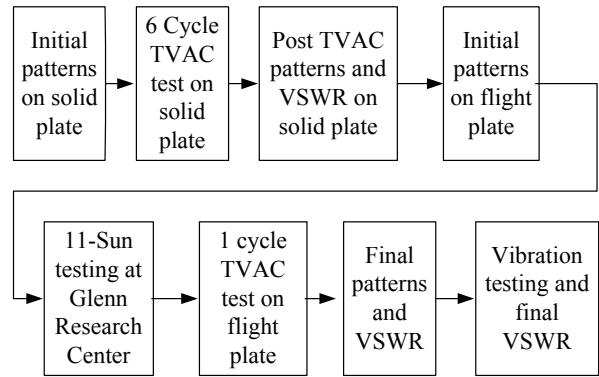


**Figure 5 Antenna Test Flow**

Array Calibration and Lookup Table Creation

In order to create an accurate lookup table with which to steer the phased-arrays, the differences in radiated phases of each waveguide stick, as well as the phase differences in the feed paths of the waveguide sticks, needed to be taken into account.

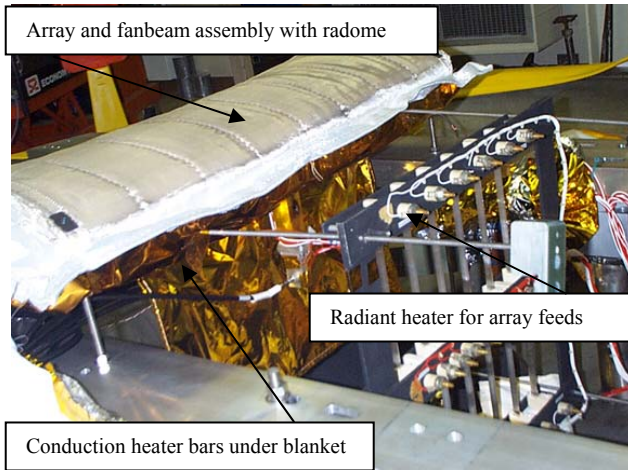


**Figure 6 Phased-Array and Radome in TVAC Test**

The relative radiated phases at boresight were extracted from the element patterns measured previously during flight qualification using the Compact Antenna Range. These radiated phases were used to determine the radiated offset vector ( $\phi_{rad}$ ), which corrects this inherent disparity in radiated phase. The non-uniformity in radiated phase is most apparent in the back array, which has waveguide right-angle bends on four of the array inputs, needed to accommodate the limited space behind the back antenna plate.

At spacecraft integration, the cable paths feeding the array sticks were also included in the calibration. The phase was measured through each path, shown in Figure 7, from each input to the hybrid coupler to each waveguide stick. These measurements were performed using a network analyzer with both SSPAs powered on and in the “0-phase state”. These measured phase differences were used to create the coax offset vector ( $\phi_{coax}$ ), needed to compensate for the phase variation across the array input feeds.

The two offset vectors were all that were needed to calibrate the array and create a lookup table of scan positions between  $-60^\circ$  and  $+60^\circ$  from boresight. The offset vectors were calculated relative to Stick 1 of each array, resulting in a 0-state phase position for Stick 1 across all scan positions, however, any of the eight sticks could be reassigned as the reference, in the case of a stuck phase-shifter bit, for example.

The phasing increment ( $\Delta$ ) in degrees for each electrical scan angle was determined through:

$$\Delta = 180 \cdot \sin(\Theta * \frac{\pi}{180})$$

where  $\Theta$  is the desired beam-steer angle.

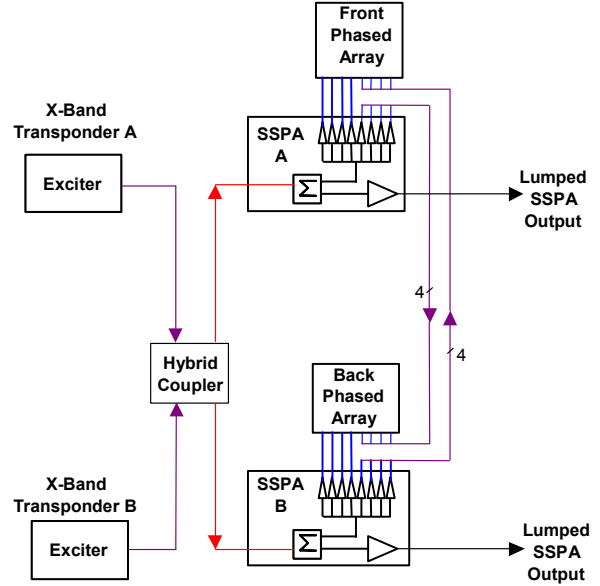


**Figure 7 Phased-Array System Calibration Paths**

The required phase state (0 to 15) for each 4-bit phase-shifter ( $22.5^\circ$  Least Significant Bit) was determined through:

$$M = MOD\left(\frac{(N-1) * \Delta - \phi_{coax} - \phi_{rad}}{22.5}, 16\right)$$

where M is an integer between 0 and 15 that represents the state of the phase shifter and N is an integer between 1 and 8 that represents the antenna stick element location.

The phase states of each of the eight sticks were then used to form the hexadecimal word which was stored in memory and used to command the arrays according to a desired scan position.

### 3. Spacecraft-Level Testing

#### Phased-Array Steering Test

Traditionally, hat coupler measurements have been used to confirm antenna performance at the spacecraft level so that one can test in the final flight configuration and yet not free radiate. In order to confirm that the MESSENGER electronically scanned array was being steered correctly, the hat coupler method required some modification.

The antenna pattern of the MESSENGER phased-array is determined by the magnitude and phase of the eight input signals and the element patterns of the eight waveguide sticks of the array. A method for monitoring the signal phase of each slotted waveguide is necessary in order to verify correct operation of the antenna system. The

monitoring method should not adversely affect the performance of the antenna, and it should be simple enough to implement when the antenna is mounted on the spacecraft.

Sampling of the RF signal in each slotted waveguide was accomplished through the use of a small loop coupler. The loop coupler was inserted through a hole in the short circuit at one end of the waveguide, so that the loop protruded slightly into the waveguide interior. Near the short circuit, the electric field is zero but the magnetic field is at a maximum. The plane of the loop was oriented orthogonal to the magnetic field vectors to maximize the magnetic flux through the loop. This time-varying magnetic flux induces a detectable voltage in the wire that forms the loop, and the voltage may be displayed on a network analyzer. Measurements of a loop coupler showed a coupling of -20 dB. The small coupling implied that the perturbation caused by the loop had a negligible effect on antenna performance. There was sufficient coupling, however, to allow for monitoring of the phase of the waveguide field.

The loop coupler, shown in Figure 8, was fabricated from 2.2-mm (0.086-inch) diameter, semi-rigid coaxial cable and a two-hole flange-mount SMA jack connector. The semi-rigid cable was soldered into the jack connector, and part of the coaxial shield and dielectric was stripped away from the other end of the cable to expose the center conductor. The center conductor was then bent into a hairpin loop and soldered to the coaxial shield. The overall length of the loop was about 6.35 mm (0.25 inch), and its diameter was less than the diameter of the coaxial cable, so it may be inserted through any hole which admits the coaxial cable. The short circuit plates in the slotted waveguides were designed so that the flange-mount SMA connector may be securely screwed to a plate, with the coupling loop extending just beyond the plate into the waveguide interior. Installation and de-installation were accomplished with the antenna mounted on the spacecraft.

The loop couplers were used during integration and testing to verify that the phased-array system was working properly. The loop couplers were monitored as shown in Figure 9 using a digitally commanded eight-way RF switch in conjunction with an HP8410 vector analyzer. The RF switch was attached to the RF absorber lined antenna hat of each array and routed to each of the eight loop couplers through semi-rigid cable and in-line attenuators. A 10 dB coupler was attached to the loop coupler output of Stick 1 to provide a reference for the vector analyzer. This reference line, the common line of the RF switch, and an 8-bit digital harness (including power to the switch) were run from inside the integration facility to the vector analyzer and digital command software (Labview) outside the facility.



**Figure 8 Loop Coupler**

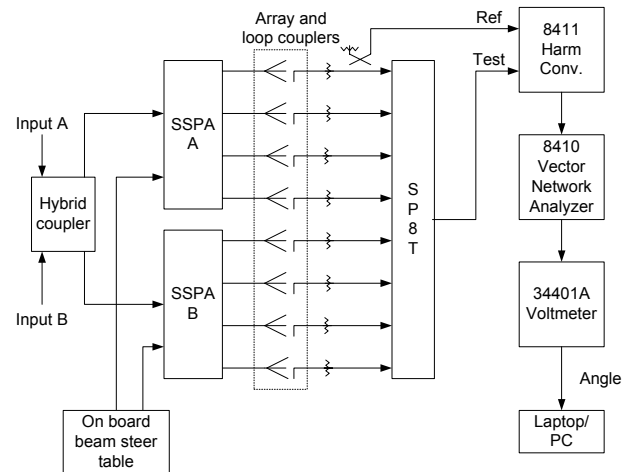


**Figure 9 Spacecraft-Level Phased-Array Test Setup**

The loop couplers were calibrated by commanding all phase shifters in both SSPAs to the “0-phase-state”. The RF switch was cycled to measure the phase of each loop coupler through the RF switch assembly, relative to the phase coupled out of the first loop coupler. Since the phase inputs to the feed of each waveguide stick had already been measured for the 0-phase-state (to determine the coax offset vector), it was simply a matter of subtracting the coax phases from the loop coupler phases measured through the switch to perform the calibration. This transfer function between loop coupler phase and the phase at the input to each of the waveguide sticks could then be used throughout phased-array testing with the antenna hat to verify performance of the phased-array system.

Throughout phased-array testing at the spacecraft level, the loop couplers were used to determine the individual stick phases using the same RF switch assembly and Labview software. A complex sum of the eight patterns was performed to provide an estimation of what the actual pattern of the array should resemble for a given scan command. This complex sum uses the individual element

radiation patterns measured previously and applies the above calibration to the monitored loop coupler phases. As a matter of convenience, the reconstructed pattern was plotted in real time to give the integration engineer a validation of the commanded scan position. The reconstructed gain envelope, based on a series of complex summations, agrees very well with measured array gain envelope as shown in Figure 10.

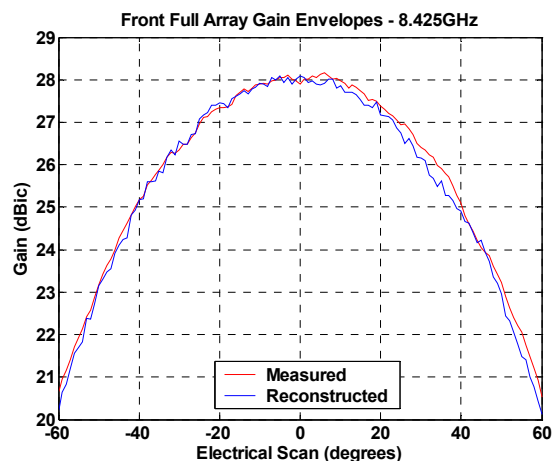


**Figure 10 Reconstructed and Measured MESSENGER Phased-Array Gain Envelope**

#### 4. Summary

Measurement techniques for the MESSENGER spacecraft phased-array antenna include compact antenna range measurements, thermal vacuum testing, and spacecraft-level testing. Two techniques for characterizing a phased-array system have been developed. The gain envelope response measurement allows one to rapidly determine the performance of a phased-array antenna in a single antenna pattern measurement. The phase steering verification technique confirms that the antenna beam is steered properly at the spacecraft level without free radiating.

#### 5. References

[1] Solomon, S. C., R. L. McNutt, Jr., R. E. Gold, M. H. Acuña, D. N. Baker, W. V. Boynton, C. R. Chapman, A. F. Cheng, G. Gloeckler, J. W. Head, III, S. M. Krimigis, W. E. McClintock, S. L. Murchie, S. J. Peale, R. J. Phillips, M. S. Robinson, J. A. Slavin, D. E. Smith, R. G. Strom, J. I. Trombka, and M. T. Zuber, The MESSENGER mission to Mercury: Scientific objectives and implementation, *Planet. Space Sci.*, 49, 1445-1465, 2001.

[2] Gold, R. E., S. C. Solomon, R. L. McNutt, Jr., A. G. Santo, J. B. Abshire, M. H. Acuña, R. S. Afzal, B. J. Anderson, G. B. Andrews, P. D. Bedini, J. Cain, A. F. Cheng, L. G. Evans, W. C. Feldman, R. B. Follas, G. Gloeckler, J. O. Goldsten, S. E. Hawkins, III, N. R. Izenberg, S. E. Jaskulek, E. A. Ketchum, M. R. Lankton, D. A. Lohr, B. H. Mauk, W. E. McClintock, S. L. Murchie, C. E. Schlemm, II, D. E. Smith, R. D. Starr, and T. H. Zurbuchen, The MESSENGER mission to Mercury: Scientific payload, *Planet. Space Sci.*, 49, 1467-1479, 2001.

[3] Santo, A. G., R. E. Gold, R. L. McNutt, Jr., S. C. Solomon, C. J. Ercol, R. W. Farquhar, T. J. Hartka, J. E. Jenkins, J. V. McAdams, L. E. Mosher, D. F. Persons, D. A. Artis, R. S. Bokulic, R. F. Conde, G. Dakermanji, M. E. Goss, Jr., D. R. Haley, K. J. Heeres, R. H. Maurer, R. C. Moore, E. H. Rodberg, T. G. Stern, S. R. Wiley, B. G. Williams, C. L. Yen, and M. R. Peterson, The MESSENGER mission to Mercury: Spacecraft and mission design, *Planet. Space Sci.*, 49, 1481-1500, 2001.

[4] R. K. Stilwell, R. E. Wallis, and M. L. Edwards, A circularly polarized, electrically scanned slotted waveguide array suitable for high temperature environments, *IEEE Antennas and Propagation Society International Symposium Proceedings*, Vol. 3, pp. 1030 - 1033, June 22-27, 2003.

[5] R. E. Wallis and S. Cheng, Phased-array antenna system for the MESSENGER deep space mission, *IEEE Aerospace Conference Technical Digest*, March 2001.

[6] Bokulic, R. S., K. B. Fielhauer, R. E. Wallis, S. Cheng, M. L. Edwards, R. K. Stilwell, J. E. Penn, J. R. Bruzzi, and P. M. Malouf, MESSENGER mission: First electronically steered antenna for deep space communications, *Proc. IEEE Aerospace Conference*, Paper 1370, CD-ROM 4-1503, Big Sky, MT, March 6-13, 2004.

#### 6. Acknowledgements

The MESSENGER program is sponsored by the NASA Office of Space Science. The authors wish to thank MESSENGER's Principal Investigator, Dr. S. C. Solomon of the Carnegie Institution of Washington, and R. S. Bokulic, S. Cheng, M. L. Edwards, L. A. Ellis, D. G. Grant, R. K. B. Fielhauer, D. W. Royster, R. C. Schulze, D. K. Srinivasan, R. K. Stilwell, and J. T. Will of JHU/APL, for their support of this work.